Measurements of C-13 Multiple-Quantum Coherences in Amyloid Fibrils under Magic-Angle Spinning

ARTICLE *in* THE JOURNAL OF PHYSICAL CHEMISTRY B · MAY 2012

Impact Factor: 3.3 · DOI: 10.1021/jp303455w · Source: PubMed

4 AUTHORS, INCLUDING:

Jerry Chan
National Taiwan University
95 PUBLICATIONS **2,412** CITATIONS

THE JOURNAL OF PHYSICAL CHEMISTRY B

Article

pubs.acs.org/JPCB

Measurements of ^{13}C Multiple-Quantum Coherences in Amyloid Fibrils under Magic-Angle Spinning

Fang-Chieh Chou, Tim W. T. Tsai, Hsin-Mei Cheng, and Jerry C. C. Chan*

Department of Chemistry, National Taiwan University, No. 1, Section 4, Roosevelt Road, Taipei, Taiwan

Supporting Information

ABSTRACT: The excitation and detection of high-order multiple quantum coherences among ^{13}C nuclear spins are demonstrated in the samples of [1-^{13}C]-L-alanine and ^{13}C labeled amyloid fibrils at a spinning frequency of 20 kHz. The technique is based on the double-quantum average Hamiltonian prepared by the DRAMA-XY4 pulse sequence. Empirically, we find that multiple supercycles are required to suppress the higher-order effects for real applications. Measurements for the fibril samples formed by the polypeptides of PrP(113−127) provide the first solid-state NMR evidence for the stacking of multiple β-sheet layers at the structural core of amyloid fibrils

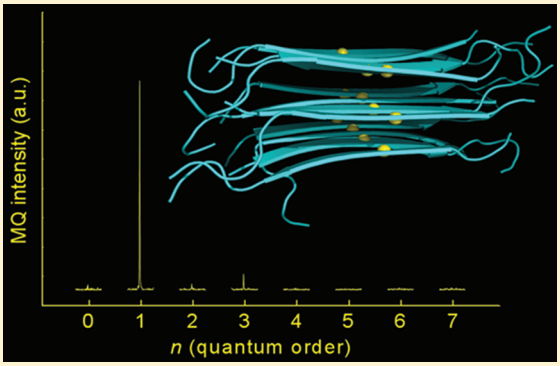

1. INTRODUCTION

Solid-state nuclear magnetic resonance (SSNMR) is nowadays an indispensable technique for the study of noncrystalline biological solids such as amyloid fibrils.[1,2] The power of recoupling techniques such as rotational resonance (R^2)[3,4] and dipolar recoupling with a windowless sequence (DRAWS)[5] were well recognized in the early studies of amyloid fibrils by SSNMR.[6,7] Since then, many novel dipolar recoupling techniques have been developed for the measurements of internuclear distances under the condition of magic-angle spinning (MAS)[8] and fruitful applications in the field of amyloid fibrils have been observed.[9] In particular, determination of the number of spins in a spin system, i.e. spin counting, may provide important structural constraints. In this regard, multiple-quantum (MQ) NMR is a powerful technique for spin counting because the observation of an n-quantum signal implies that there must be at least n spins coupled in a spin network.[10] A controlled evolution of the intramolecular MQ signals may also be exploited to determine torsion angles.[11] The first application of MQ NMR to the study of amyloid fibrils was carried out under static condition,[12] where signals up to 5Q were observed for two singly labeled Aβ_{1-40} fibril samples (Ala21-$^{13}C^{\beta}$ and Ala30-$^{13}C^{\beta}$). These observations have firmly established that the β-sheet structure of the Aβ_{1-40} fibrils is in-register parallel.[12] However, it is highly desirable to detect MQ coherences under the high-resolution condition provided by MAS. In addition, MQ NMR measurements for C′ under static condition are very inefficient because of the large chemical shift anisotropy. To tackle these problems, Oyler and Tycko have developed the technique of high-speed magic-angle spinning multiple quantum (HSMAS-MQ), where the finite-pulse RFDR (fpRFDR) sequence is incorporated into some MQ NMR techniques developed for static solids.[13] In the presence of chemical shift difference, the effective Hamiltonian of fpRFDR has a spin part which is a linear combination of the spherical tensor operators of $T_{2,0}$ and $T_{0,0}$. Therefore, the time reversal condition, which is important for the observation of MQ coherences, may be difficult to achieve for HSMAS-MQ method under certain circumstances. Furthermore, the down-scaling of the effective Hamiltonian would lead to a substantially longer excitation time. Double-quantum Hamiltonian could be employed for better MQ excitation efficiency as demonstrated in the work by Kristinsen et al. using the sequence of SR26.[14] Alternatively, one may also exploit the second-order recoupling effect for the efficient excitation of 3Q coherence.[15,16] However, these methods are not applicable in the regime of moderate MAS (ca. 20 kHz). In this work, we show that the pulse sequence of DRAMA-XY4[17,18] can be employed for the excitation of MQ coherences under moderate MAS conditions. Experimentally, we have verified the utility of our approach by detecting the MQ signals up to 7Q for [1-^{13}C]-L-alanine at a spinning frequency of 20 kHz. Applications to the study of the fibril samples formed by the sequence fragment of the prion protein ($PrP_{113-127}$) show that there are at least three tightly stacking β-sheet layers at the fibril core region.

2. THEORY

2.1. DRAMA-XY4. As shown before, the practicability of DRAMA can be greatly enhanced by incorporating four π pulses with XY-4 phases into the basic DRAMA cycles.[17,18] The resulting sequence with the acronym of DRAMA-XY4 has a

Received: April 10, 2012
Revised: May 24, 2012
Published: May 25, 2012

larger scaling factor than fp-RFDR and therefore it should be more efficient in MQ excitation. To obtain a pure DQ Hamiltonian to the lowest order, the sequence of DRAMA-XY4 can be flanked by a pair of $\pi/2$ pulses and the hence obtained DQ Hamiltonian has the following form:[18]

$$H_D^{(1)} = \frac{3}{\pi\sqrt{2}} d_{12} \sin(2\beta_{PR}) \cos(\gamma_{PR})(I_{1x}I_{2x} - I_{1y}I_{2y}) \quad (1)$$

where β_{PR} and γ_{PR} are the Euler angles bringing the principal axis system of the dipolar tensor to the rotor-fixed coordinate. For the observation of MQ signals with coherence order higher than two, it is crucial to have a sign change between the effective Hamiltonians of the excitation and reconversion blocks,[10,13] which can be easily achieved in our case by phase shifting the reconversion block by $\pi/2$. With this so-called time reversal property, the destructive interference among the MQ coherences could be avoided. However, a straightforward application of the pulse sequence shown in Figure 1 did not

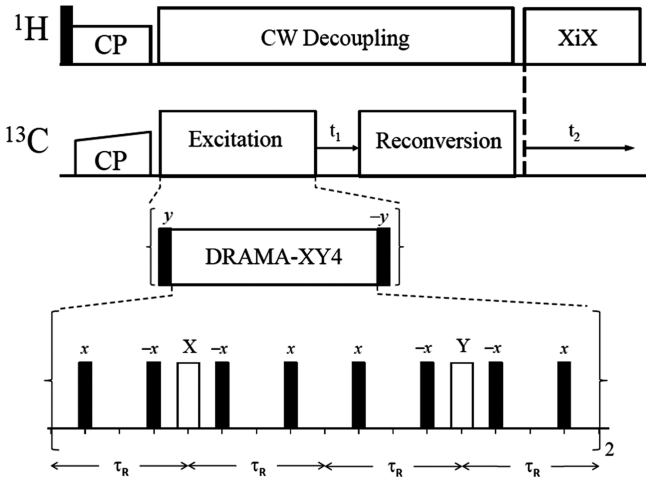

Figure 1. Pulse sequence employed for MQNMR experiments. The pulse blocks of the excitation and reconversion differ by an overall phase shift of $\pi/2$ to fulfill the time reversal condition. The rf phases for the $\pi/2$ (filled rectangles) and π pulses (open rectangles) of the basic DRAMA-XY4 cycle are shown in lower- and upper-case letters, respectively. The subscript 2 of the curly brackets denotes a repeat of the enclosed items. The pulse sequence shown here is used for the excitation of odd-order MQ coherences. To excite the even-order coherences, a ^{13}C $\pi/2$ pulse could be inserted after the CP period to create a longitudinal magnetization before the MQ excitation block, while another reading pulse could be added right before the acquisition period. In practice, we simply removed the first flanking $\pi/2$ pulse of the excitation block and the second flanking $\pi/2$ pulse of the reconversion block.

produce any appreciable signals of 3Q or higher. The difficulties are mainly due to the effects of pulse imperfection, resonance offset, chemical shift anisotropy, which are detrimental to the time reversibility of the effective Hamiltonian. As discussed earlier, it is possible to improve the robustness of a pulse sequence by carefully designed supercycles.[19−21] The formal theory of supercycles based on phase shifting and phase inversion has been discussed in detail.[14] Recently, a very general treatment of symmetry principles of NMR pulse sequences has been presented by Levitt, where a set of compact operators were used to describe a comprehensive collection of various symmetry expansions of pulse cycles.[22] Although the topic of supercycles was not covered in depth, one may envision many new possible designs of supercycles on the basis of the symmetry concepts discussed therein. Below we will give an exposition of the supercycles we designed to improve the robustness of DRAMA-XY4.

2.2. Design of Supercycles. Under the condition of MAS, the high-field Hamiltonian of a spin 1/2 system takes the following form:

$$H(t) = H_{rf}(t) + H_{\text{int}}(t) = H_{rf}(t) + \sum_{\Lambda,\lambda,L,m} \omega_{L,m}^{\Lambda} \exp(-im\omega_R t) T_{\lambda 0}^{\Lambda}, \quad (2)$$

where Λ represents various internal interactions, $\omega_{L,m}^{\Lambda}$ are the orientation-dependent coefficients of the Fourier components of the spatial functions ($-2 \le m \le 2$), and $T_{\lambda,0}^{\Lambda}$ are irreducible tensor operators of rank λ. Consider the supercycle constructed by expanding the basic DRAMA-XY4 cycle based on the following condition (Figure 2a):

(a)

$$[\,x\bar{x}\ X\ \bar{x}x - x\bar{x}\ Y\ \bar{x}x\,]_2 - [\,\bar{x}x\ \bar{Y}\ x\bar{x} - \bar{x}x\ \bar{X}\ x\bar{x}\,]_2$$

(b)

$$[\,\bar{x}x\ \bar{X}\ x\bar{x} - \bar{x}x\ \bar{Y}\ x\bar{x}\,]_2 - [\,x\bar{x}\ Y\ \bar{x}x - x\bar{x}\ X\ \bar{x}x\,]_2$$

(c)

$$[\,\bar{x}x\ \bar{X}\ x\bar{x} - \bar{x}x\ Y\ x\bar{x}\,]_2 - [\,x\bar{x}\ \bar{Y}\ \bar{x}x - x\bar{x}\ X\ \bar{x}x\,]_2$$

$$[\,x\bar{x}\ X\ \bar{x}x - x\bar{x}\ \bar{Y}\ \bar{x}x\,]_2 - [\,\bar{x}x\ Y\ x\bar{x} - \bar{x}x\ \bar{X}\ x\bar{x}\,]_2$$

Figure 2. Supercycles designed to stabilize the performance of the DRAMA-XY4 sequence. (a) First bracketed entries represent the short-hand notation of the basic rf phases described in Figure 1. The overbar indicates a negative rf phase. The second bracketed group of rf phases represents the supercycle prepared by the antipalindromic expansion of the first one. (b) Another supercycle created by phase shifting all the rf pulses by π. (c) The rf phases of the third level of supercycle are obtained by a π rotation of all the preceding rf phases along the y-axis. The overall supercycle formed by concatenating the schemes shown in parts a−c spans a total of 64 rotor periods.

$$H_{rf}(t) = -H_{rf}(-t) \text{ for } -t_C \le t \le t_C \quad (3)$$

where t_C is the duration of the basic cycle (i.e., $t_C = 8\ \tau_R$). This supercycle conforms to the so-called antipalindromic expansion of pulse sequence[22] and it has been commonly employed in homonuclear decoupling experiments under static conditions.[23] Accordingly, the propagator of the rf field from the time points $-t$ to 0 is given as

$$U_{rf}(0, -t) = \hat{T} \exp[-i \int_{-t}^{0} dt'\ H_{rf}(t')] \quad (4)$$

where $\hat{T}$ is the Dyson time ordering operator. By substituting $t' = -t''$ into the above equation, we obtain

$$U_{rf}(0, -t) = \hat{T} \exp[i \int_{t}^{0} dt''\ H_{rf}(-t'')] \quad (5)$$

dx.doi.org/10.1021/jp303455w | J. Phys. Chem. B 2012, 116, 7162−7167

Combining eqs 3 and 5:

$$U_{rf}(0, -t) = \hat{T} \exp[i \int_0^t dt'' H_{rf}(t'')] = U_{rf}^{-1}(t, 0) \quad (6)$$

That is, the overall propagator of the supercycle must be cyclic

$$U_{rf}(t_C, 0)U_{rf}(0, -t_C) = 1 \quad (7)$$

in spite of the fact that the individual propagator of the basic cycle could be rendered noncyclic by experimental imperfections. The first-order average Hamiltonian in the interaction frame transformed by the rf field is calculated for the period from $-t_C$ to 0 as

$$\bar{H}^{(1)}_{-t_C \to 0} = \frac{1}{t_C} \int_{-t_C}^{0} dt' \, U_{rf}^{-1}(t', -t_C) H_{int}(t') U_{rf}(t', -t_C) \quad (8)$$

Given that

$$U_{rf}(0, t)U_{rf}(t, -t_C) = U_{rf}(0, -t_C) = 1 \quad (9)$$

we can write

$$U_{rf}(t, -t_C) = U_{rf}^{-1}(0, t) \quad (10)$$

Hence,

$$\bar{H}^{(1)}_{-t_C \to 0} = \frac{1}{t_C} \int_{-t_C}^{0} dt' \, U_{rf}(0, t') H_{int}(t') U_{rf}^{-1}(0, t') \quad (11)$$

By substituting $t' = -t''$ and incorporating eq 6 into the above equation, we obtain

$$\begin{aligned} \bar{H}^{(1)}_{-t_C \to 0} &= \frac{1}{t_C} \int_0^{t_C} dt'' \, U_{rf}(0, -t'') H_{int}(-t'') U_{rf}^{-1}(0, -t'') \\ &= \frac{1}{t_C} \int_0^{t_C} dt'' \, U_{rf}^{-1}(t'', 0) H_{int}(-t'') U_{rf}(t'', 0) \\ &= \frac{1}{t_C} \int_0^{t_C} dt'' \, U_{rf}^{-1}(t'', 0) H_{int}(t'') U_{rf}(t'', 0) \\ &= \bar{H}^{(1)}_{0 \to t_C} \end{aligned} \quad (12)$$

That is, the overall average Hamiltonian of the supercycle is identical to that of the original cycle. To derive eq 12, we have assumed the validity of the condition for even function:

$$H_{int}(-t'') = H_{int}(t'') \quad (13)$$

The truncated Hamiltonian of an internal interaction under MAS comprises the cosine and sine modulations of the $\omega_r t$ term, rendering the above condition invalid for the most general cases. For the DRAMA pulse sequence, however, only the $\cos(\omega_r t)$ term of H_{int} (t) is relevant (Supporting Information). Consequently, eqs 13 and 12 are justified in our case. Experimentally, we have found that this supercycle created by antipalindromic expansion is mandatory for the excitation of MQ coherences by DRAMA-XY4 (data not shown).

As shown in Figure 2b, another supercycle was created by phase shifting all pulse elements by π. The advantage of this π-shifted supercycle has been well documented[14] and requires no further elaboration here. The final step of our supercycle is obtained by a π rotation along the y-axis (Figure 2c), which is discussed in the following treatment. For simplicity, we focus on the chemical shift interaction only. When a supercycle is generated by a π rotation along an arbitrary axis on the xy plane, the new propagator is calculated as:

$$U'_{rf}(t) = \Pi_\phi^{-1} U_{rf}(t) \Pi_\phi \quad (14)$$

where

$$\Pi_\phi = \exp[-i\pi(\cos\phi I_x + \sin\phi I_y)] \quad (15)$$

In the interaction frame transformed by the rf field, we have

$$\begin{aligned} \tilde{H}'_{CS}(t) &= \Pi_\phi^{-1} U_{rf}^{-1}(t, 0) \Pi_\phi H_{CS}(t) \Pi_\phi^{-1} U_{rf}(t, 0) \Pi_\phi \\ &= -\Pi_\phi^{-1} U_{rf}^{-1}(t, 0) H_{CS}(t) U_{rf}(t, 0) \Pi_\phi \\ &= -\Pi_\phi^{-1} \tilde{H}_{CS}(t) \Pi_\phi \end{aligned} \quad (16)$$

Thus, the nth order Average Hamiltonian is calculated as:

$$\bar{H}'^{(n)}_{CS} = (-1)^n \Pi_\phi^{-1} \bar{H}^{(n)}_{CS} \Pi_\phi \quad (17)$$

For the regular phase inversion, which corresponds to the case of $\phi = 0$, the supercycle will suppress the I_y and I_z components of the second-order $(n = 2)$ chemical shift interaction. Experimentally, however, we find that the supercycle created by setting $\phi = \pi/2$ can significantly improve the robustness of the pulse sequence, which may be ascribed to the cancellation of the I_x and I_z components of the second-order terms.

2.3. Detection of MQ Coherences. In principle, one can differentiate the MQ coherences of different orders by a systematic increment of the rf phases of the initial state and the excitation sequence. Because of the limitation of our instrumental setup, we chose to resolve the MQ signals by evolution under resonance offset (see Figure 1). Because the t_1 increment was set equal to a rotor period, the spectral window usable to accommodate the excited MQ coherences would have an effective bandwidth of $\nu_R/2$. Given that the maximum evolution time in the t_1 dimension is $15\tau_R$, the maximum MQ order that could be observed without aliasing is calculated as $(\nu_R/2)/(\nu_R/15) - 0.5 = 7$. Because a two-spin double-quantum average Hamiltonian is created in our pulse sequence, the detected MQ signals should be of either odd or even orders, depending on whether the longitudinal or transverse spin magnetization is prepared as the initial spin state. This coherence order selection can reduce considerably the data acquisition time because in real applications the observation of a particular coherence order may be sufficient to verify the fidelity of a structural model. Take the cross-β motif of amyloid fibrils for an instance, the organization of in-register parallel β-sheet structure will lead to the observation of ^{13}C 3Q coherence for a sample labeled at a single site.[13]

3. EXPERIMENTAL METHODS

[1-^{13}C]-L-alanine was used as received from Cambridge Isotope Laboratories (Andover, USA). $PrP_{113-127}$ peptides, with the sequence Ac-AGAAAAGAVVGGLGG-NH_2, were synthesized on an automated Odyssey microwave peptide synthesizer (CEM Corp., Matthews, USA). ^{13}C- and ^{15}N-labeled amino acids with FMOC protection were obtained from Cambridge Isotope Laboratories (Andover, USA), CortecNet (Tilleuls, France), and Isotec (St. Louis, USA). The details of sample preparation were described elsewhere.[24] For the fibril sample of

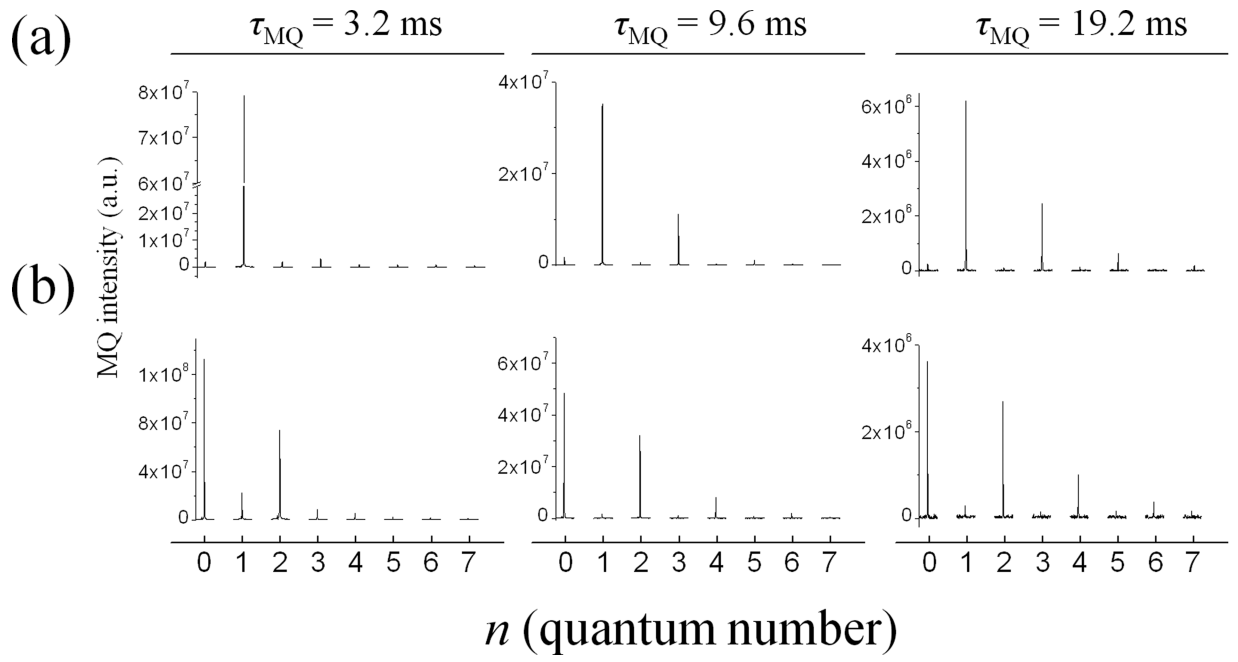

Figure 3. MQNMR experiments measured for [1-^{13}C]-L-alanine. The sample mass is ~10 mg. (a) Detection of the odd-quantum signals. Number of transients accumulated is 64. Spectrometer time is ~1.1 h. (b) Detection of the even-quantum signals. Number of transients accumulated is 128.

COCO, the carbonyl carbons of Ala117 and Ala120 were ^{13}C enriched, whereas the carbonyl carbons of Ala118 and the methyl carbons of Ala113 were ^{13}C enriched for the COCB sample. All NMR experiments were carried out at ^{13}C, and ^{1}H frequencies of 75.5, and 300.1 MHz, respectively, on a Bruker DSX300 spectrometer equipped with a commercial 2.5-mm double-resonance probe. The measurements were carried out at ambient temperature. Each sample was packed in the middle one-third of the rotor volume using Teflon spacers. The magic-angle spinning (MAS) was carried out at a frequency of 20 kHz and its variation was limited to ±3 Hz using a commercial pneumatic control unit (Bruker, MAS II). A contact time of 1.5 ms was used for the ^{13}C{^{1}H} cross-polarization, where the ^{1}H rf field was set to 50 kHz and that of ^{13}C was adiabatically ramped through the Hartmann−Hahn matching condition.[25] During the DRAMA-XY4 recoupling period, the ^{13}C π pulses were set to 8 μs. The ^{13}C $\pi/2$ pulses flanking the DRAMA-XY4 pulse blocks were set to 4 μs. Continuous-wave proton decoupling of 130 kHz was applied during the recoupling period. Proton decoupling of 100 kHz was applied during the t_2 acquisition using the scheme of XiX.[26] Recycle delay was set to 4 s. The tachometer signals for pulse sequence synchronization were filtered with a home-built phase-locked loop circuit. For the measurements of the COCB sample, the MQ excitation of the carbonyl and methyl signals were carried out in two separate experiments where the transmitter frequency was applied next to the resonance position of the target signal.

For the measurements of the MQ spectra, the t_1 increment was set equal to a rotor period. Typically, a total of 16 data points were acquired in the t_1 dimension, corresponding to a maximum evolution time of 15τ_R. Accordingly, an offset of ν_R/15 was given to the peak of interest. The MQ intensities were calculated by the Fourier transformation of the signals with respect to t_1 using MATLAB.[27] The amplitudes of the MQ coherences were calculated from the moduli of the complex signals after the transformation.

4. RESULTS AND DISCUSSION

4.1. Crystalline Model Compound. As an experimental verification, we measured the ^{13}C MQ NMR spectra for [1-^{13}C]-L-alanine at a spinning frequency of 20 kHz. The odd and even orders of MQ coherences were excited separately. For the odd-quantum spectra, signals up to 7Q were observed as the excitation time increased from 3.2 to 19.2 ms (Figure 3a). In particular, the excitation efficiency of the 3Q coherence, normalized by the CPMAS signal, was found to be 2.1%, 7.8%, and 1.7% when the MQ excitation time was set to 3.2, 9.6, and 19.2 ms, respectively. As experimental artifacts, some residual even-quantum signals were observed at short excitation time. These undesirable artifacts are presumably due to the flip-angle imperfections of the $\pi/2$ pulses. Nonetheless, such artifacts become negligible for long excitation time, at which the most interesting high-order MQ coherences are excited. Comparable results were obtained for the even-quantum spectra but the signal artifacts are more severe (Figure 3b). Therefore, we chose to measure the odd-quantum signals for the fibril samples (*vide infra*). Recently, an efficient excitation of ^{13}C MQ signal has been achieved using a well compensated sequence SR26.[14] However, the rf field required for SR26 is 6.5 times the MAS frequency. Therefore, it is difficult to apply SR26 at a spinning frequency of 20 kHz as in our case.

4.2. Fibrils Formed by Fragment of Human Prion Protein. The molecular structure of amyloid fibrils are known to contain β-sheets formed by intermolecular hydrogen bonding of neighboring β-strand peptide strands that run perpendicular to the fibril axis. The interstrand distance is ~5 Å. As an illustration for real applications in biological samples, we apply the DRAMA-XY4 technique to study the amyloid fibrils formed by the fragment of prion protein $PrP_{113-127}$. Previously, we have shown that the $PrP_{113-127}$ fibrils adopt the antiparallel β-sheet organization, where the residue 117 + k forms backbone hydrogen bonds to residue 120 − k in $PrP_{113-127}$ fibrils.[24] That is, the carbonyl carbons of the residues 117 and 120 would form an extended chain of spins with

dx.doi.org/10.1021/jp303455w | J. Phys. Chem. B 2012, 116, 7162−7167

internuclear distance of ~5 Å. For the COCO sample, the carbonyl carbons of Ala117 and Ala120 were ^{13}C enriched. Accordingly, MQ coherences up to 3Q were observed for the COCO sample (Supporting Information). Although the observation of higher-order coherences (> 3Q) in fibril samples under MAS condition remains very difficult, the detection of 3Q coherence may be sufficient to provide invaluable constraints for the molecular structure of amyloid fibrils.

Recently, Eisenberg and co-workers have suggested that a unique packing mode between the neighboring β-sheet layers could be found in amyloid fibrils.[28,29] The term "steric zipper" is coined to describe the dry surface between two tightly interdigitated β-sheets. In particular, a total of eight classes of steric zipper have been categorized, reflecting the various relative orientations of the two stacking β-sheet layers.[29] Previously, we have shown that $PrP_{113-127}$ fibrils adopt the structural motif of the class 7 steric zipper.[24] That is, the two stacking antiparallel β sheets have the same orientation along the fibril axis. However, the experimental data reported therein cannot rule out the possibility that there are more than two β-sheet layers stacking to form the core structure. In a coarse-grain modeling of the fibrillization process of polyalanine,[30] it has been shown that the β-sheet elongation mechanism would take over when the nucleation site contains multiple β-sheet layers (typically six). Figure 4 shows the MQ spectrum

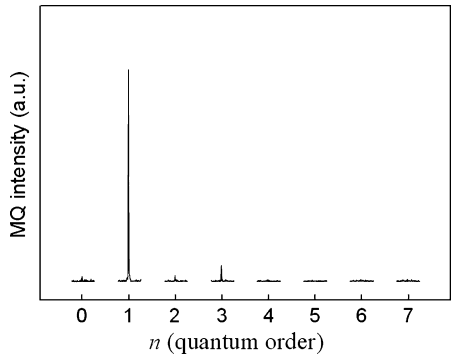

Figure 4. ^{13}C odd-quantum MQNMR spectrum measured for the carbonyl signals of the COCB sample. The excitation time was set to 22.4 ms. The sample mass is 5.0 mg. Number of transients accumulated is 640.

obtained for the carbonyl signals of the COCB sample, in which the carbonyl carbons of Ala118 and the methyl carbons of Ala113 were ^{13}C enriched. In addition to the fact that the residues of Ala118 and Ala113 are distant by more than 7 Å, DRAMA is a band-selective technique and therefore the MQ excitation of C′ will not be interfered by any neighboring $^{13}C^{\beta}$ spins. On the basis of the structural motif of class 7 steric zipper, the observation of the 3Q signal provides an unequivocal evidence for the stacking of more than two β-sheet layers. As a result, our data lend considerable support to the fibrillization model proposed by Hall and co-workers.[30] It is also legitimate to suggest that the steric zipper motif, which comprises only two stacking β sheets, should be revised to accommodate the scenarios of multiple stacking β sheets.

To the best of our knowledge, this work represents the first successful excitation of MQ coherence across multiple β-sheet layers, which is a direct consequence of the fact that the distance between two interdigitated β-sheet layers is comparable to the interstrand distance of the individual β sheet for the alanine zipper formed by polypeptides containing the palindromic sequence AGAAAAGA.[24,31,32] Finally, we found it difficult to detect the MQ signals for the methyl carbons, which may be due to the detrimental effects of the relatively fast spin–lattice relaxation of Ala113-C^{β}.

4. CONCLUSIONS

We have developed an efficient technique based on DRAMA-XY4 for the excitation of ^{13}C MQ coherences under magic-angle spinning conditions. Although the design of the basic pulse sequence is rather straightforward, we find that it is mandatory to apply judiciously designed supercycle to suppress the higher-order effects for real applications. Our method has the favorable feature that it can be applied at moderately fast spinning regime and experimentally we have verified the fidelity of our approach at a spinning frequency of 20 kHz. Excitation of 3Q coherence has been obtained for the $PrP_{113-127}$ fibrils, from which we have obtained compelling evidence for the stacking of more than two β-sheet layers at the core region of the fibrils.

■ ASSOCIATED CONTENT

Ⓢ Supporting Information

Time modulations of the spin and spatial parts of the homonuclear dipolar Hamiltonian and ^{13}C odd-quantum MQNMR spectrum. This material is available free of charge via the Internet at http://pubs.acs.org.

■ AUTHOR INFORMATION

Corresponding Author

*Telephone: 886-2-3366 2994. Fax: 886-2-2363 6359. E-mail: chanjcc@ntu.edu.tw.

Notes

The authors declare no competing financial interest.

■ ACKNOWLEDGMENTS

This work was supported by grants from the National Science Council.

■ REFERENCES

(1) Tycko, R. *Q. Rev. Biophys.* **2006**, *39*, 1.
(2) Heise, H. *ChemBioChem* **2008**, *9*, 179.
(3) Raleigh, D. P.; Levitt, M. H.; Griffin, R. G. *Chem. Phys. Lett.* **1988**, *146*, 71.
(4) Levitt, M. H.; Raleigh, D. P.; Creuzet, F.; Griffin, R. G. *J. Chem. Phys.* **1990**, *92*, 6347.
(5) Gregory, D. M.; Wolfe, G. M.; Jarvie, T. P.; Sheils, J. C.; Drobny, G. P. *Mol. Phys.* **1996**, *89*, 1835.
(6) Lansbury, P. T.; Costa, P. R.; Griffiths, J. M.; Simon, E. J.; Auger, M.; Halverson, K. J.; Kocisko, D. A.; Hendsch, Z. S.; Ashburn, T. T.; Spencer, R. G. S.; Tidor, B.; Griffin, R. G. *Nat. Struct. Biol.* **1995**, *2*, 990.
(7) Gregory, D. M.; Benzinger, T. L. S.; Burkoth, T. S.; Miller-Auer, H.; Lynn, D. G.; Meredith, S. C.; Botto, R. E. *Solid State Nucl. Magn. Reson.* **1998**, *13*, 149.
(8) Ladizhansky, V. *Solid State Nucl. Magn. Reson.* **2009**, *36*, 119.
(9) Chan, J. C. C. Solid State NMR Techniques for the Structural Determination of Amyloid Fibrils. *Top. Curr. Chem.* **2012**, *306*, 47.
(10) Weitekamp, D. P.; Waugh, J. S. Time-Domain Multiple-Quantum NMR. *Adv. Magn. Reson.* **1983**, 111.
(11) Eden, M.; Brinkmann, A.; Luthman, H.; Eriksson, L.; Levitt, M. H. *J. Magn. Reson.* **2000**, *144*, 266.
(12) Antzutkin, O. N.; Balbach, J. J.; Leapman, R. D.; Rizzo, N. W.; Reed, J.; Tycko, R. *Proc. Natl. Acad. Sci. U.S.A.* **2000**, *97*, 13045.

(13) Oyler, N. A.; Tycko, R. *J. Phys. Chem. B* **2002**, *106*, 8382.
(14) Kristiansen, P. E.; Carravetta, M.; van Beek, J. D.; Lai, W. C.; Levitt, M. H. *J. Chem. Phys.* **2006**, *124*, 234510.
(15) Eden, M. *Chem. Phys. Lett.* **2002**, *366*, 469.
(16) Eden, M.; Brinkmann, A. *J. Magn. Reson.* **2005**, *173*, 259.
(17) Klug, C. A.; Zhu, W. L.; Merritt, M. E.; Schaefer, J. *J. Magn. Reson. A* **1994**, *109*, 134.
(18) Chou, F.-C.; Tsai, T. W. T.; Lee, H.-K.; Chan, J. C. C. *Solid State Nucl. Magn. Reson.* **2009**, *36*, 177.
(19) Levitt, M. H. Symmetry-based pulse sequence in magic-angle spinning solid-state NMR. In *Encyclopedia in Nuclear Magnetic Resonance*, Grant, D. M., Harris, R. K., Eds. Wiley: Chichester, U.K., 2002; Vol. *9*, pp 165.
(20) Brinkmann, A.; Schmedt auf der Günne, J.; Levitt, , M. H. *J. Magn. Reson.* **2002**, *156*, 79.
(21) Brinkmann, A.; Eden, M. *J. Chem. Phys.* **2004**, *120*, 11726.
(22) Levitt, M. H. *J. Chem. Phys.* **2008**, *128*, 052205.
(23) Haeberlen, U. High Resolution NMR in Solids: Selective Averaging. In *Advances in Magnetic Resonance, Supplement 1*, Waugh, J. S., Ed. Academic Press: New York, 1976.
(24) Cheng, H.-M.; Tsai, T. W. T.; Huang, W. Y. C.; Lee, H.-K.; Lian, H.-Y.; Chou, F.-C.; Mou, Y.; Chan, J. C. C. *Biochemistry* **2011**, *50*, 6815.
(25) Hediger, S.; Meier, B. H.; Ernst, R. R. *Chem. Phys. Lett.* **1995**, *240*, 449.
(26) Ernst, M.; Samoson, A.; Meier, B. H. *J. Magn. Reson.* **2003**, *163*, 332.
(27) *MatLab*, 5.3.0; Mathworks, Inc.: Natick, MA, 1999.
(28) Nelson, R.; Sawaya, M. R.; Balbirnie, M.; Madsen, A. O.; Riekel, C.; Grothe, R.; Eisenberg, D. *Nature* **2005**, *435*, 773.
(29) Sawaya, M. R.; Sambashivan, S.; Nelson, R.; Ivanova, M. I.; Sievers, S. A.; Apostol, M. I.; Thompson, M. J.; Balbirnie, M.; Wiltzius, J. J. W.; McFarlane, H. T.; Madsen, A. O.; Riekel, C.; Eisenberg, D. *Nature* **2007**, *447*, 453.
(30) Nguyen, H. D.; Hall, C. K. *Proc. Natl. Acad. Sci. U.S.A.* **2004**, *101*, 16180.
(31) Lee, S. W.; Mou, Y.; Lin, S.-Y.; Chou, F.-C.; Tseng, W.-H.; Chen, C.-h.; Lu, C.-Y. D.; Yu, S. S.-F.; Chan, J. C. C. *J. Mol. Biol.* **2008**, *378*, 1142.
(32) Walsh, P.; Simonetti, K.; Sharpel, S. *Structure* **2009**, *17*, 417.